

1-1-1988

# Metastable bcc mischmetal-magnesium alloys

Antonio Sabariz  
*Iowa State University*

Follow this and additional works at: <https://lib.dr.iastate.edu/rtd>

 Part of the [Metallurgy Commons](#)

---

## Recommended Citation

Sabariz, Antonio, "Metastable bcc mischmetal-magnesium alloys" (1988). *Retrospective Theses and Dissertations*. 18603.  
<https://lib.dr.iastate.edu/rtd/18603>

This Thesis is brought to you for free and open access by the Iowa State University Capstones, Theses and Dissertations at Iowa State University Digital Repository. It has been accepted for inclusion in Retrospective Theses and Dissertations by an authorized administrator of Iowa State University Digital Repository. For more information, please contact [digirep@iastate.edu](mailto:digirep@iastate.edu).

Metastable bcc mischmetal-magnesium alloys

by

Antonio Luiz R. Sabariz

A Thesis Submitted to the  
Graduate Faculty in Partial Fulfillment of the  
Requirements for the Degree of  
MASTER OF SCIENCE

Department: Materials Science and Engineering  
Major: Metallurgy

---

Signatures have been redacted for privacy

Iowa State University  
Ames, Iowa

1988

## ABSTRACT

The bcc phase in the MM-Mg system can be metastably retained at room temperature for magnesium composition within the range 16 at.% - 20 at.%. The retention of a lower composition was restricted by quenching rate and at higher concentrations by intermetallic compound precipitation.

The lattice parameter for the pure bcc mischmetal phase was determined by extrapolation. The value obtained ( $a_E = 4.131 \text{ \AA}$ ) was in good agreement with the theoretical value ( $a_t = 4.156 \text{ \AA}$ ). Magnetic susceptibility data suggested that bcc mischmetal-magnesium alloys underwent a change from paramagnetic to antiferromagnetic behavior on cooling at  $\sim 20 \text{ K}$ , independent of magnesium composition. The value found for the magnetic effective moment per gram-atom-magnetic-rare earth of each bcc MM-Mg alloy examined (MM - 16 Mg, MM - 18 Mg and MM - 20 Mg) was found to be constant ( $p_{\text{eff}} \approx 1.62 \mu_B$ ), independent of the magnesium composition. The observed Curie-Weiss temperature values decreasing with the magnesium content increasing were due to magnetic dilution.

The equilibrium reaction  $\text{bcc} \rightarrow \text{dhcp} + \text{MMg}$  presented an undercooling effect of  $\sim 40^\circ\text{C}$  around the eutectoid composition ( $\sim 17 \text{ at.}\% \text{ Mg}$ ). The sluggish character of this reaction was considered the strongest effect for the bcc structure retention in the mischmetal-magnesium system.

## TABLE OF CONTENTS

	Page
INTRODUCTION	1
CONDITIONS FOR THE BCC MISCHMETAL HIGH TEMPERATURE PHASE RETENTION	2
EXPERIMENTAL PROCEDURES	5
RESULTS	9
DISCUSSION	41
CONCLUSIONS	44
REFERENCES	45
ACKNOWLEDGMENTS	47
APPENDIX A: MISCHMETAL CHEMICAL COMPOSITION	48
APPENDIX B: ALLOY CALCULATION	49
APPENDIX C: CALCULATED PURE BCC MISCHMETAL LATTICE PARAMETER	50

## INTRODUCTION

It is known that among the rare earth elements, many transform to the body-center cubic (bcc) structure at high temperatures [1]. Scientists at Ames Laboratory found it was possible to retain the bcc high temperature phase by alloying the rare earth element with magnesium and quenching from the liquid state. Gibson and Carlson [2] studied the Y-Mg system, Miller and Daane [3] investigated the heavy rare earth-Mg systems and more recently, Manfrinetti and Gschneidner [4] and Herchenroeder [5] worked with the La-Mg, Gd-Mg and Dy-Mg alloys. Some work was also done in the mischmetal-magnesium system by Fishman and Crowe [6] at the Naval Weapons Laboratory.

Pure mischmetal (MM) is basically a lanthanum-cerium-praseodymium-neodymium metallic alloy. It is known that MM has a bcc high temperature phase [7], and it was also verified that this phase can be retained at room temperature for at least the MM - 19 at.% Mg composition [6].

In order to determine the composition range of magnesium that is suitable for the retention of the bcc phase, several samples were quenched and analyzed utilizing X-ray diffraction and metallography. Some of the physical and magnetic properties, such as lattice parameter and magnetic susceptibility, were measured for several compositions. From plots of the physical property vs. composition, the values for the pure bcc MM phase were determined by extrapolation. Also, the equilibrium phase diagram for the mischmetal rich region was determined.

# CONDITIONS FOR THE BCC MISCHMETAL HIGH TEMPERATURE PHASE RETENTION

Pure mischmetal has a high temperature bcc phase [7]. For the mischmetal used in this investigation, the bcc phase exists from 804°C to 883°C (melting point). The high temperature of transformation (804°C) and the large energy of transformation ( $\Delta H_{Tr} \approx 3.07$  KJ/mol) [8] make the bcc phase transform to the dhcp phase isothermally. Large  $\Delta H_{Tr}$  means only a small amount of subcooling occurs before the dhcp forms and the high temperature of transformation does not permit the undercooled bcc from freezing in. An alloy element is needed to expand the bcc field and also lower the transition temperature for the bcc  $\rightarrow$  dhcp transformation. Magnesium was found to be one of the elements that best combines the alloy theory requirements and the needs for the bcc retention, as can be seen in Table 1 and Figure 1, respectively.

Kinetic considerations are also important. When fast cooling from the bcc state to below the eutectoid temperature, a temperature below the  $T_0$  temperature must be reached sufficiently fast to retain the bcc

Table 1. Hume-Rothery rules for extensive solid solubility

	Theory	MM-Mg system
Size factor	$\leq \pm 15\%$	13.7%
Electronegativity difference	$< \pm 0.40$	-0.11

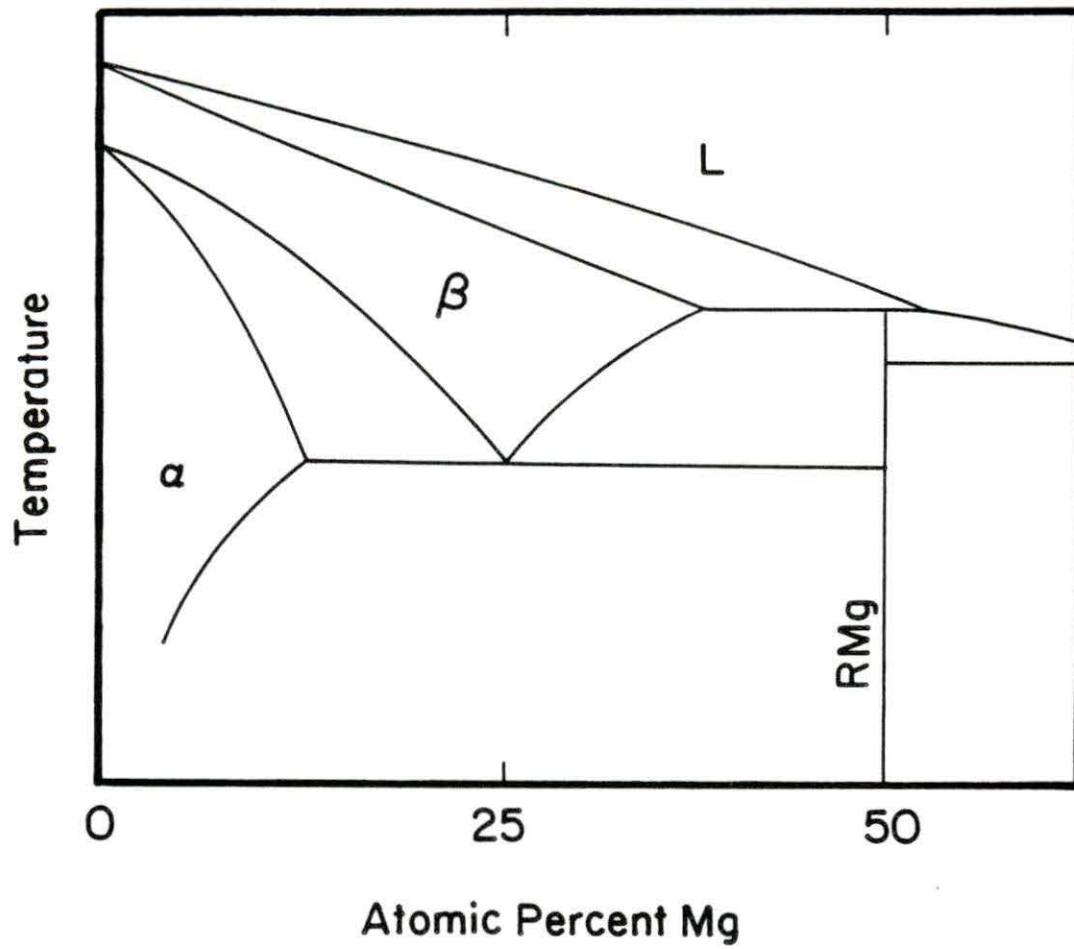


Figure 1. Typical rare earth-Mg (RE rich end) phase diagram [9]



phase. The  $T_0$  temperature is the temperature at which the dhcp and bcc phase free energies are the same in the bcc + dhcp two-phase region. An important condition for high temperature phase retention in an alloy system is that the critical temperature (which is defined as the  $T_0$  value for the lowest composition for which it is possible to retain bcc) must be greater than the eutectoid transformation temperature. Herchenroeder [5] found the critical temperature for the RE-Mg systems on the average to be 515°C.



## EXPERIMENTAL PROCEDURES

### Materials

The mischmetal was prepared at the Materials Preparation Center of the Ames Laboratory. The process was described by Palmer et al. [7]. The chemical composition of the MM and the nonmetallic impurity content are given in Appendix A. The magnesium was purified by double vacuum distillation from commercial stock and was 99.998% pure.

The mischmetal was available as 2 cm diameter bars, but in order to fit the MM in the small crucibles, it was necessary to arc melt, cut and finally swage the MM to the desired final diameter. After the MM had been fabricated, it was electropolished in a 6% perchloric acid/methanol bath at -60°C, and stored in a vacuum desiccator to prevent further oxidation. The magnesium was available as small crystals and further operations were not necessary.

### Crucibles

Two kinds of crucibles were used, one for quenching studies and the other for differential thermal analyses. Both were made by welding thin-walled tantalum tubes under helium partial pressure as described by Miller et al. [10]. The crucible dimensions were 6 mm diameter, 35 mm length and 0.2 mm wall thickness for the quenching studies, and 1.5 cm diameter, 8.0 cm length and 0.2 cm wall thickness for differential thermal analyses (D.T.A.). All crucibles were outgassed in a high vacuum system ( $10^{-6}$  torr) at 1600°C for 30 minutes using induction heating.

### Alloy Preparation

The weighted amounts of mischmetal and magnesium were inserted into the crucibles and then sealed under helium partial pressure. The designated and actual compositions are given in Appendix B. The melting operation was done by using the same system used for outgassing the crucibles. The samples were melted by heating to  $\sim 980^{\circ}\text{C}$  ( $\sim 100^{\circ}\text{C}$  above the pure mischmetal melting point) for 30 minutes using an induction furnace. The temperature was checked by using an optical pyrometer. In order to obtain good homogeneity, the samples were inverted and melted again.

### Quenching

In order to protect the tantalum crucibles containing the MM-Mg alloys, they were sealed inside of a quartz capsule under partial pressure of argon. The capsules were placed in an open-air resistance furnace set at  $980^{\circ}\text{C}$  and left for 24 hours. The samples were quenched by quickly removing the capsules from the furnace and at the same time, they were broken over an ice-water-acetone bath.

### Sample Preparation

The ends of the tantalum crucible were cut first, then the crucibles were sectioned along the length by using a low-speed diamond saw, and finally, the tantalum was peeled off. The resulting samples were about  $12 \times 5 \times 1$  mm.

### X-ray Diffraction

The bulk samples were mechanically polished using 600 grit paper and then electropolished to remove the cold worked surface. The X-ray studies were done by using a diffractometer. The radiation used was  $K\alpha Cu$ ; the samples were spun to reduce preferential orientation, and scanned at a rate of  $2^\circ/\text{min}$ .

### Metallography

A technique similar to that described by Peterson and Hopkins [11] was used to prepare the sample for microscopic examination. The samples were first mechanically polished using 200 through 600 grit paper, which was followed by using a fine powder suspension of aluminum oxide and methanol. Finally, they were etched by dipping the samples into a solution of 6% perchloric acid in methanol for about 20 seconds.

### Magnetic Susceptibility

The magnetic susceptibilities of the quenched samples were measured using a Faraday magnetometer similar to that described by Croat [12]. The calibration procedure is described by Herchenroeder [5]. The susceptibility measurements were made in applied magnetic field of 1.4 T over the temperature range from 1.7 K to room temperature.

### Differential Thermal Analyses (D.T.A.)

The equipment and method used were described previously by Spedding et al. [13]. The equipment consists of a molybdenum block

where two crucibles were inserted, one containing the MM-Mg alloy and the other containing a reference metal (lutetium). The system is heated by a tantalum resistance furnace enclosed in a vacuum chamber ( $10^{-5}$  torr). The temperature and the differential temperature between the two samples were measured by a Pt - Pt 13% Rh thermocouple and recorded on a strip chart recorder.

## RESULTS

X-ray and metallographic examination attested that the MM bcc phase can be retained by quenching MM-Mg alloys within the composition range 16 at.% - 20 at.% Mg.

## X-ray Diffraction (Quenched Alloy)

The X-ray diffraction pattern of the MM - 15 at.% Mg alloy showed a mixture of retained bcc plus the equilibrium dhcp phase and the MMMg intermetallic compound (Figure 2). The presence of the bcc phase and the intermetallic compound MMMg are seen in the X-ray diffraction pattern for the MM - 21 at.% Mg alloy (Figure 3). The X-ray diffraction patterns for the alloy MM - 16 at.% Mg, MM - 18 at.% Mg and MM - 20 at.% Mg showed only the presence of the bcc phase as observed in Figures 4, 5 and 6, respectively.

From the X-ray diffraction data, the lattice parameters for the bcc retained alloys were calculated. This calculation was done by applying the Cohen method [14]. The results are shown in Table 2.

Table 2. Lattice parameters for the retained bcc alloys

Alloy	Lattice parameter
MM - 16 Mg	$4.069 \pm 3 \text{ \AA}$
MM - 18 Mg	$4.064 \pm 3 \text{ \AA}$
MM - 20 Mg	$4.054 \pm 3 \text{ \AA}$



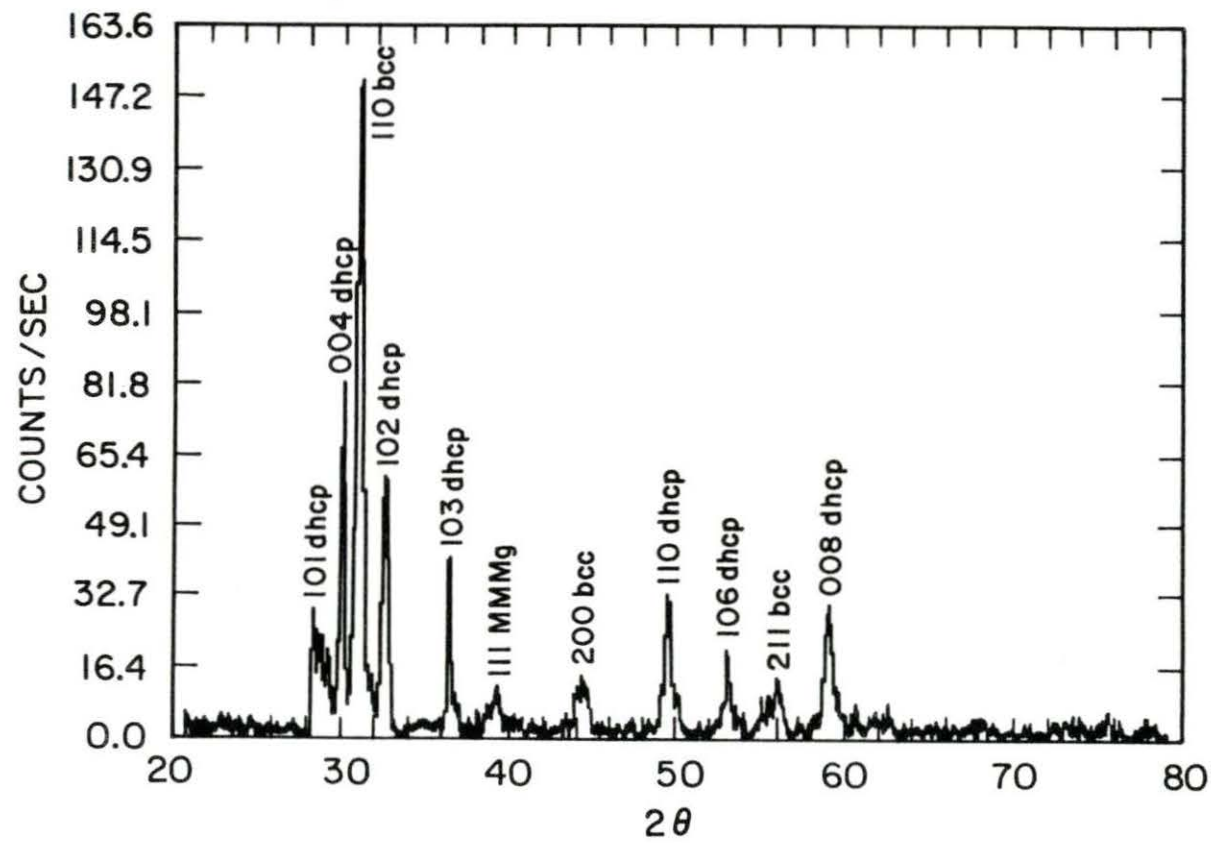


Figure 2. X-ray diffraction pattern of MM - 15 Mg alloy quenched

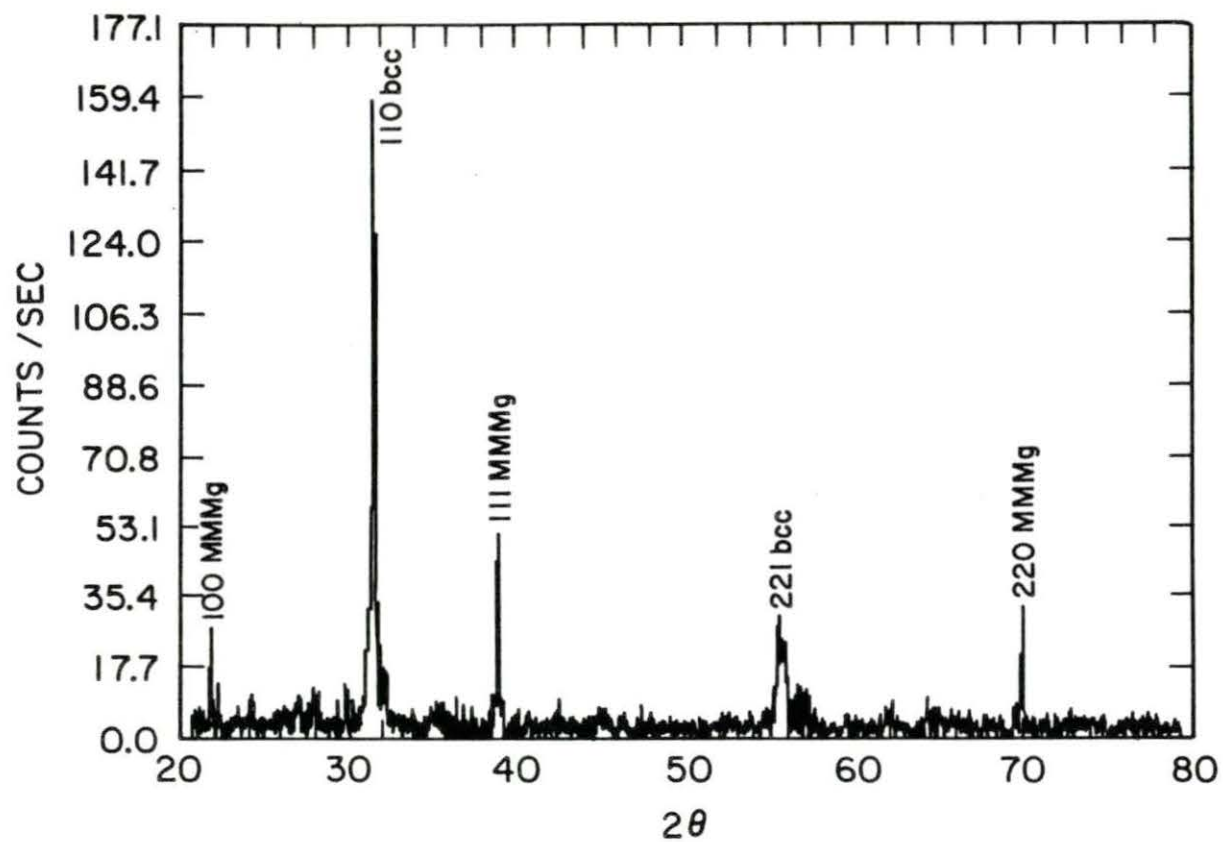


Figure 3. X-ray diffraction pattern of MM - 21 Mg alloy quenched



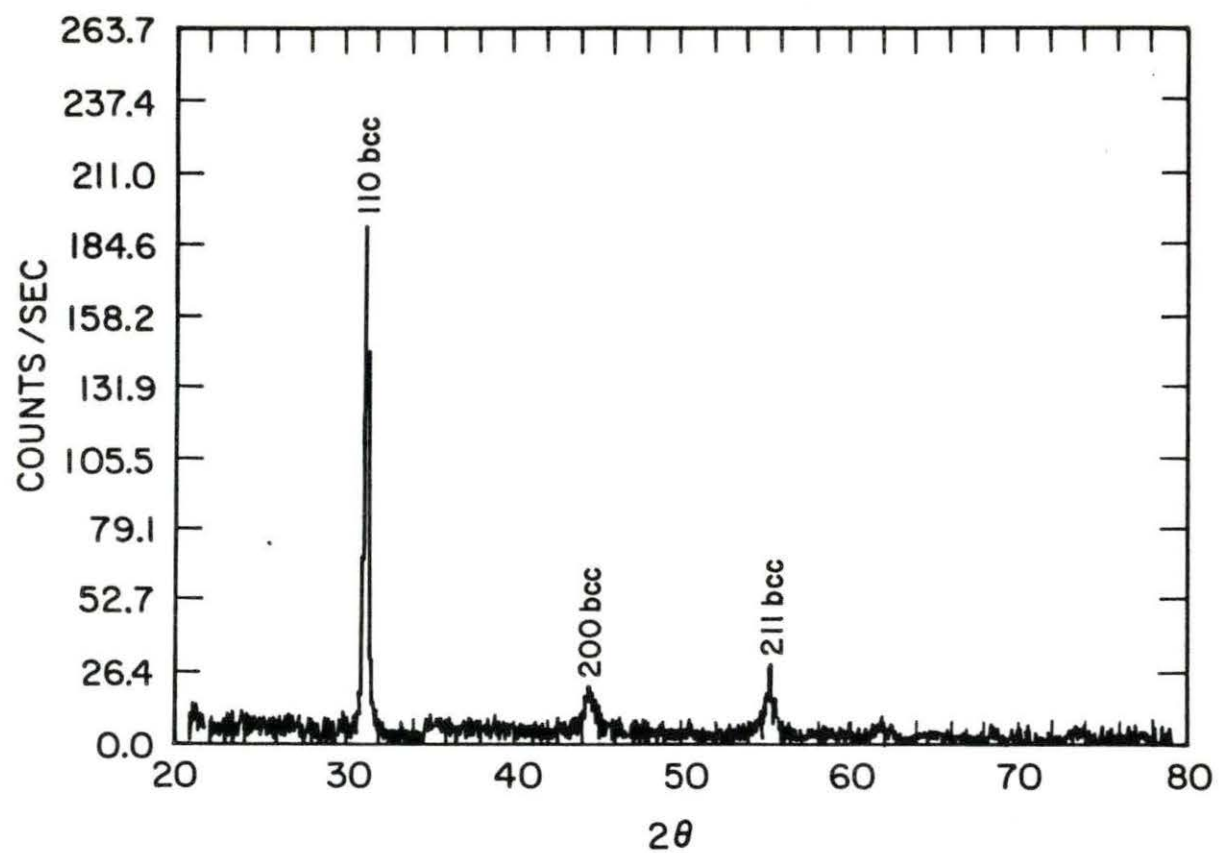


Figure 4. X-ray diffraction pattern of MM - 16 Mg alloy quenched

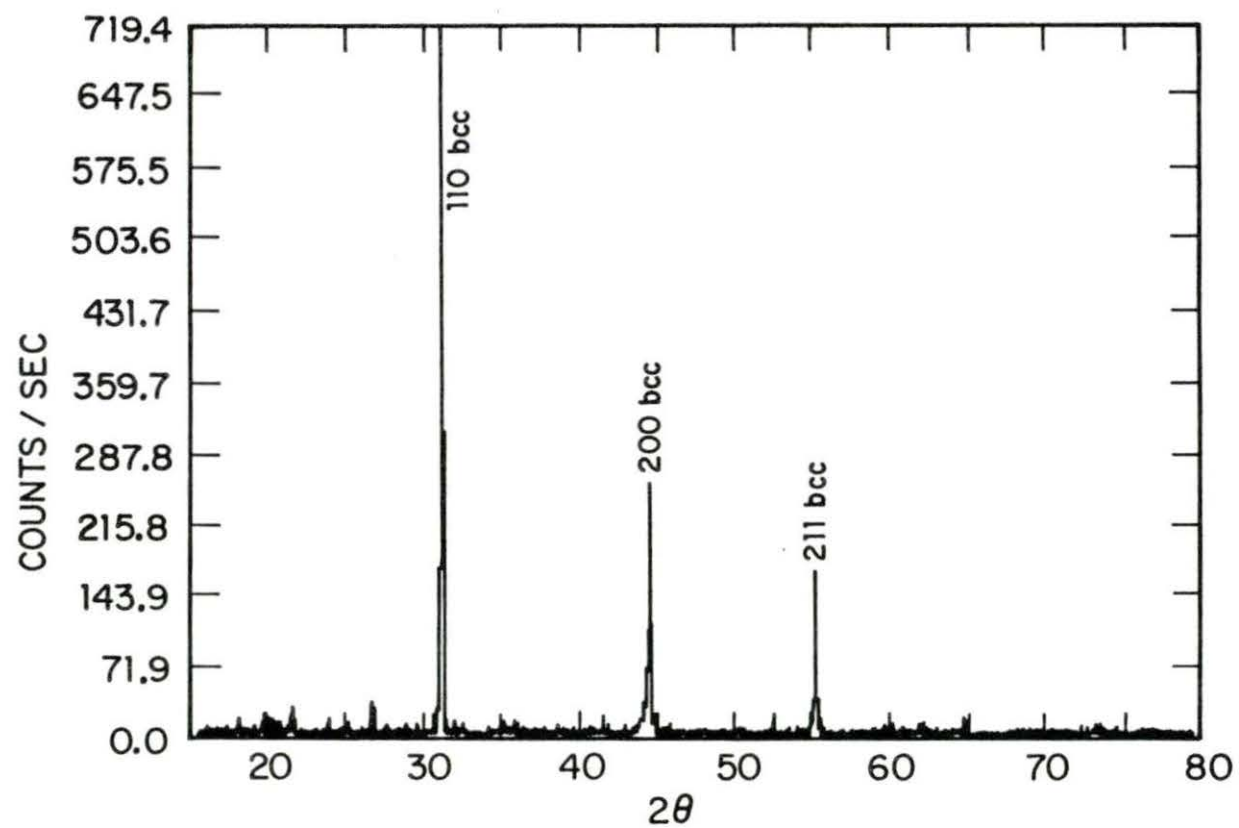


Figure 5. X-ray diffraction pattern of MM - 18 Mg alloy quenched

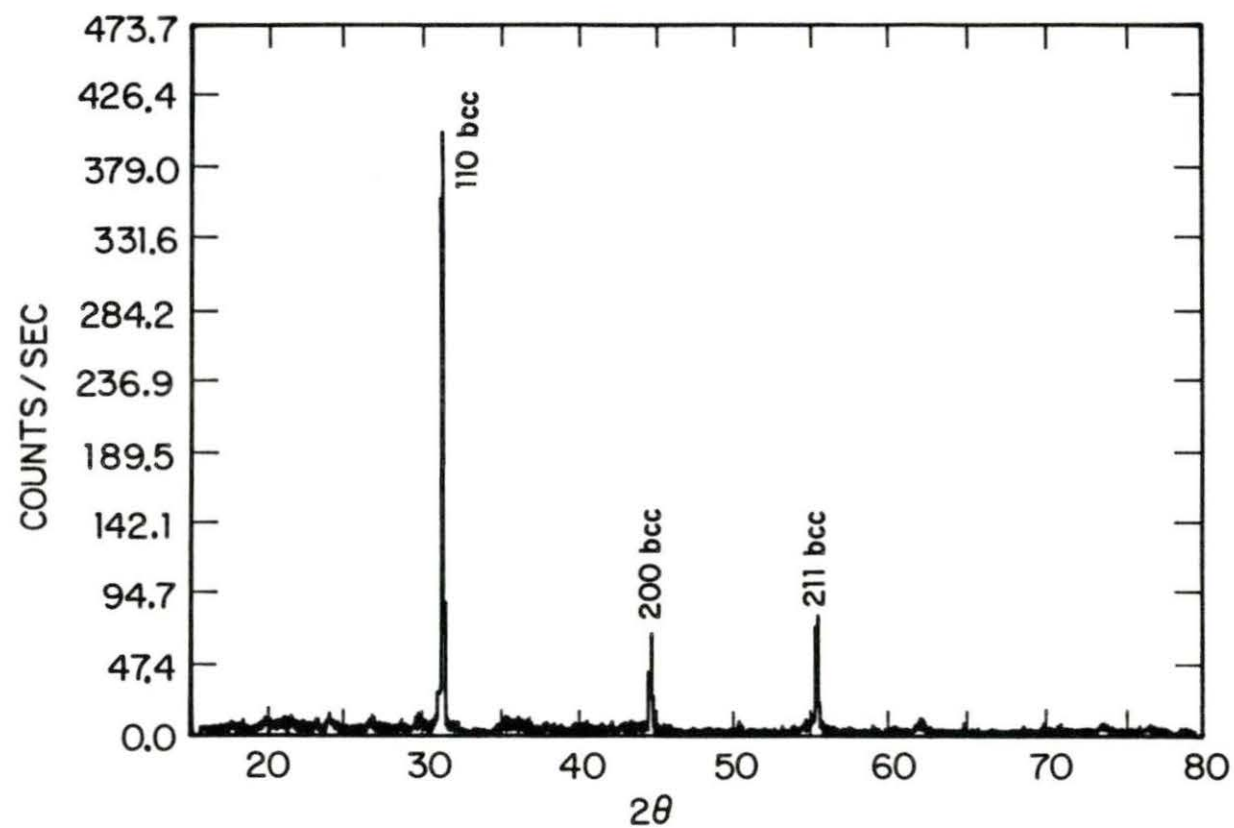


Figure 6. X-ray diffraction pattern of MM - 20 Mg alloy quenched

In order to determine experimentally the lattice parameter for the pure bcc mischmetal phase, these lattice constants were plotted against magnesium composition (Figure 7). By extrapolation to 0 at.% Mg, using the method of least squares [14], the lattice parameter of "pure MM bcc" was determined to be  $a_E = 4.131 \text{ \AA}$ . The theoretical value (detailed calculations are given in Appendix C) is  $a_T = 4.156 \text{ \AA}$ . The difference between the two values is 0.6%.

### Microstructures (Quenched Alloys)

The metallographic work confirmed the X-ray results. Figure 8(a) shows an optical micrograph of MM - 15 at.% Mg alloy, where all three phases, dhcp, bcc and the intermetallic compound MMMg are present. Figure 8(b) shows an optical micrograph of MM - 21 at.% Mg alloy, where the presence of the bcc phase and the MMMg intermetallic compound are seen. The presence of only a single phase is evident in the micrographs of MM - 16 at.% Mg, MM - 18 at.% Mg and MM - 20 at.% Mg alloys (Figures 9(a), (b) and (c), respectively).

### Magnetic Susceptibility

The magnetic susceptibility was measured for the retained bcc alloys. From the inverse susceptibility plotted against the temperature (Figures 10-12), some observations can be made. paramagnetic behavior for temperatures above  $\approx 20 \text{ K}$  is observed for all three alloys, i.e., they follow the Curie-Weiss law. On cooling, the plots suggested that bcc MM orders antiferromagnetically at  $\sim 20 \text{ K}$ .

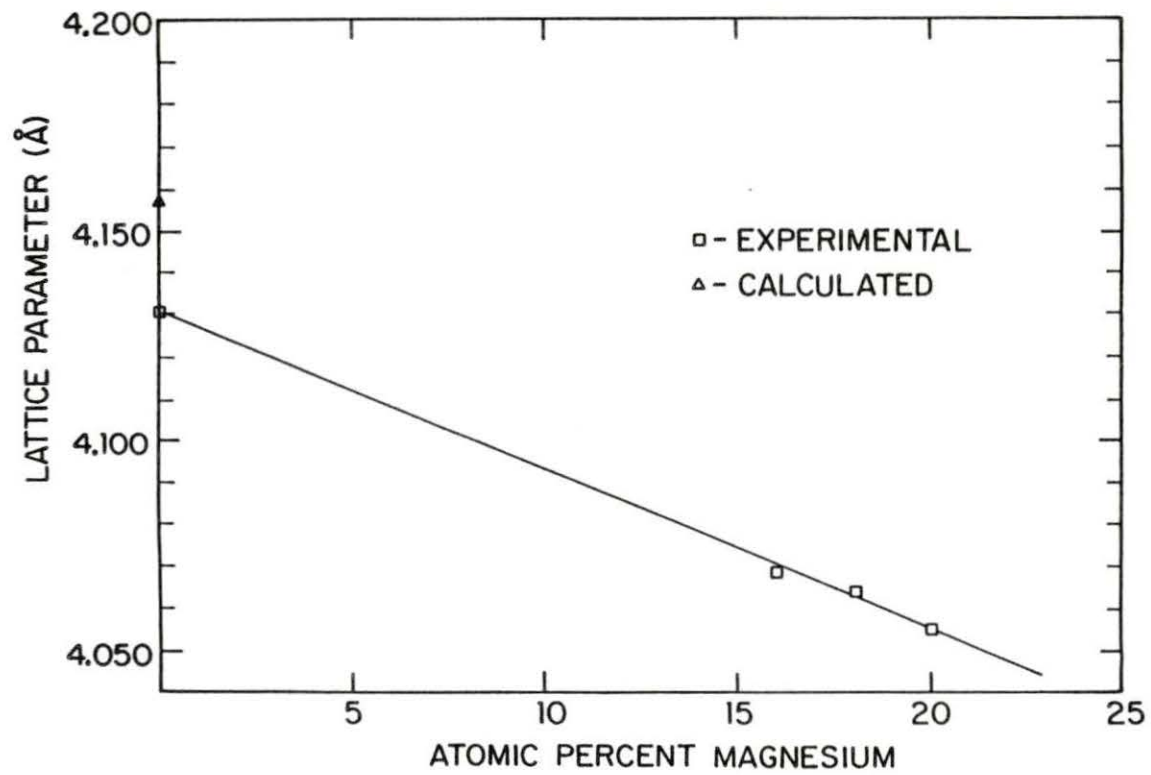
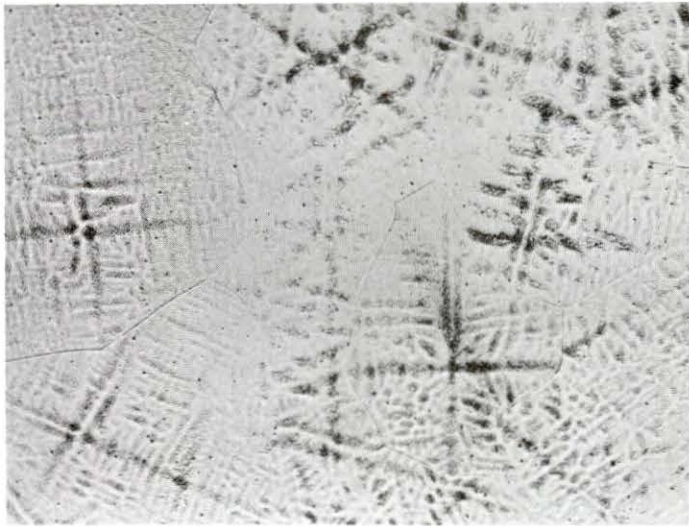
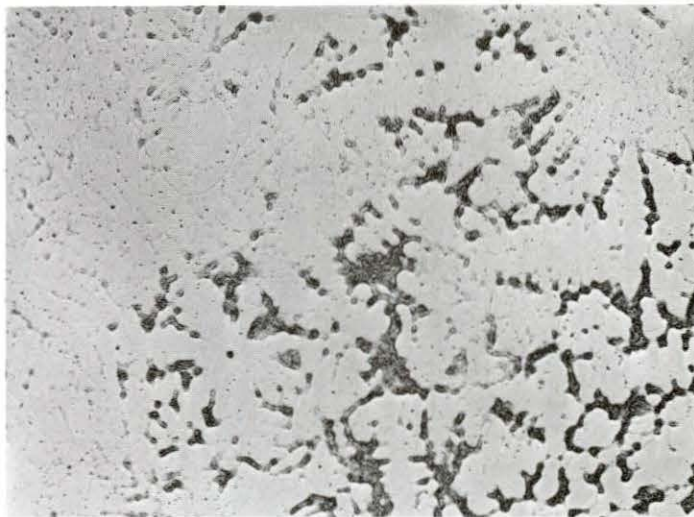


Figure 7. Lattice parameters for the bcc mischmetal - magnesium alloys



(a)



(b)

Figure 8. Optical micrographs (250X) of (a) MM - 15 Mg alloy quenched showing a dendritic structure of dhcp + MMMg in a bcc matrix and (b) MM - 21 Mg alloy quenched showing precipitation of MMMg intermetallic compound in a bcc matrix



(a)



(b)



(c)

Figure 9. Optical micrographs (250X) of (a) MM - 16 Mg, (b) MM - 18 Mg and (c) MM - 20 Mg alloys quenched, showing only retained bcc structure. The black dots are probably due to surface oxidation



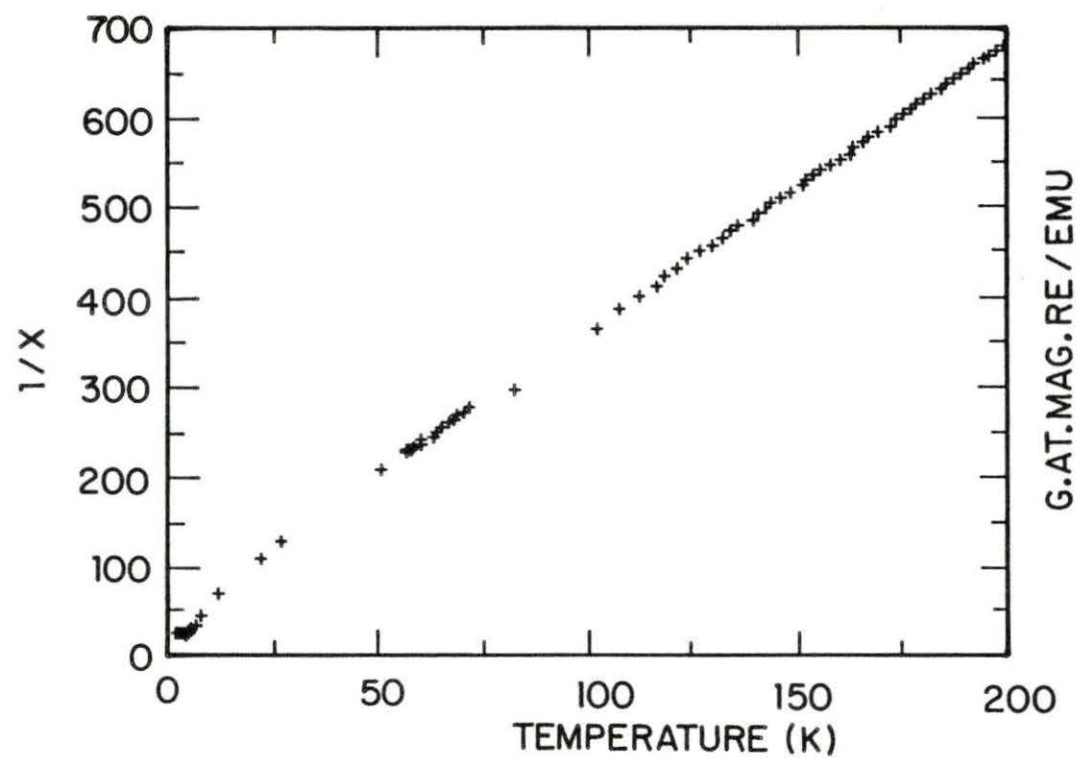


Figure 10. Inverse magnetic susceptibility for sample bcc MM - 16 Mg

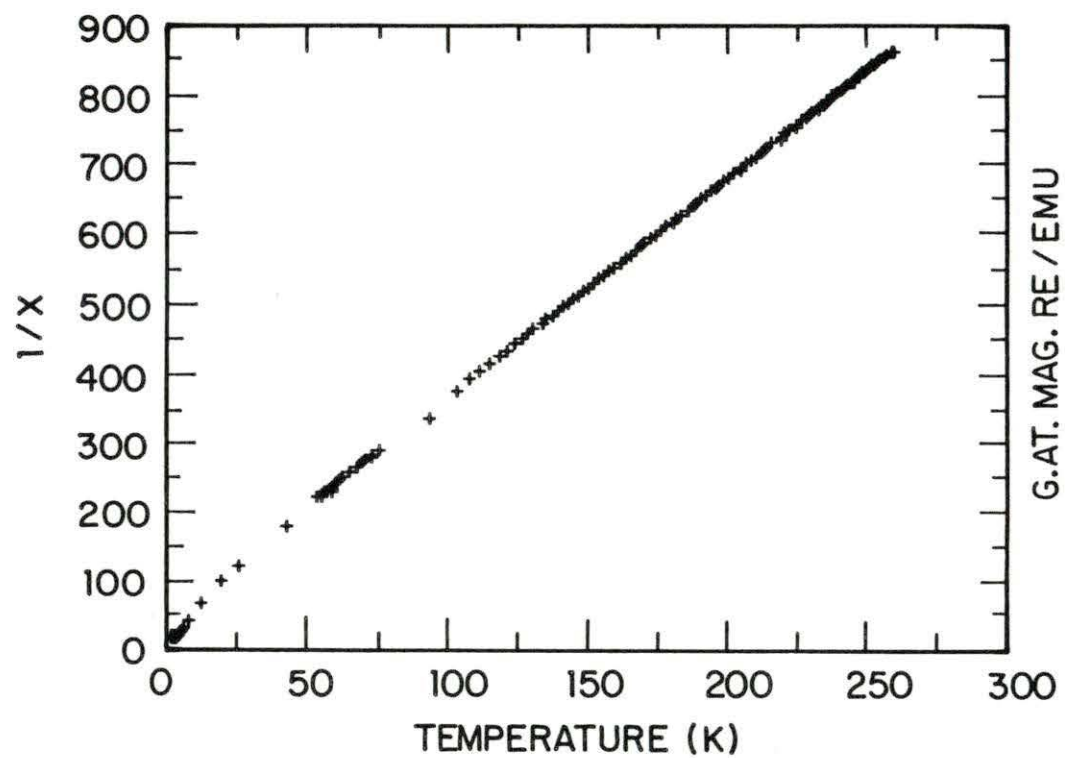


Figure 11. Inverse magnetic susceptibility for sample bcc MM - 18 Mg

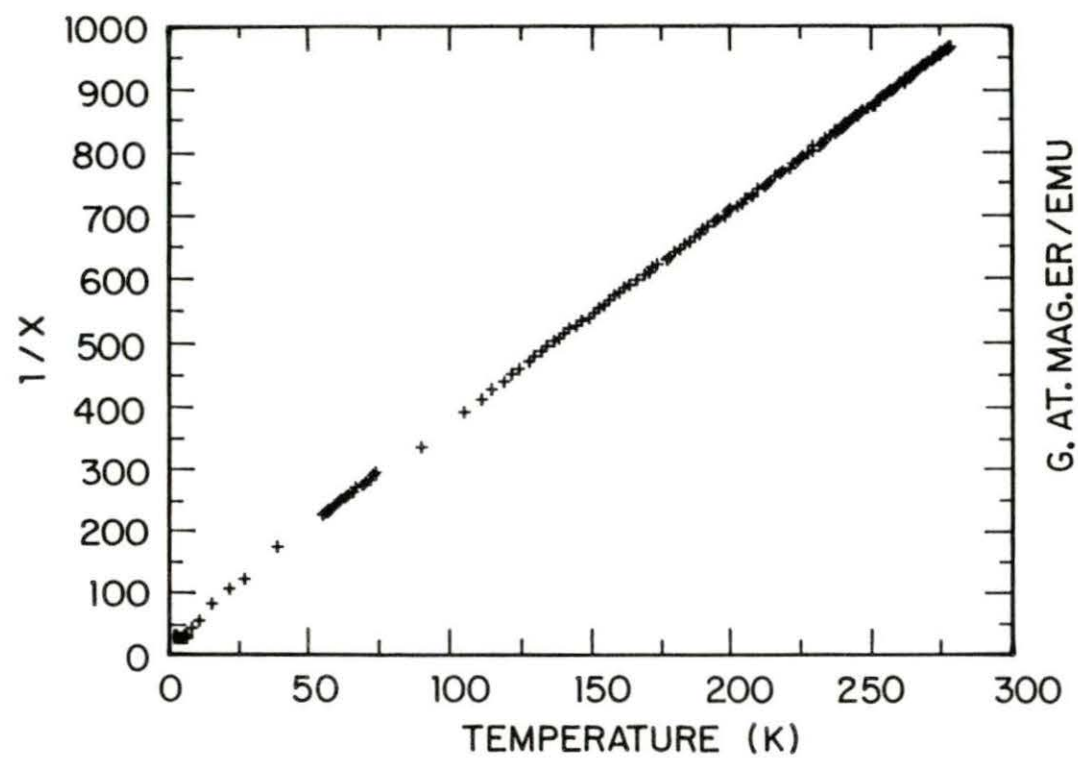


Figure 12. Inverse magnetic susceptibility for sample bcc MM - 20 Mg

The effective magnetic moments were calculated from the paramagnetic-region slope. The Curie-Weiss temperatures are given by the intercept of the least-square fit of the straight line with the temperature axis. The results are summarized in Table 3.

Table 3. Magnetic effective moment and Curie-Weiss temperatures for the MM-Mg-bcc alloys

Alloy	$\mu_{\text{eff}}$ ( $\mu_B$ ) experimental	$\mu_{\text{eff}}$ ( $\mu_B$ ) theoretical	$\Theta$ (K)
MM - 16 at.% Mg	1.615	1.620	-20.0
MM - 18 at.% Mg	1.650	1.620	-19.0
MM - 20 at.% Mg	1.612	1.620	-16.1

#### Mischmetal - Magnesium Phase Diagram (0 - 50 at.% Mg)

The MM - Mg phase diagram from 0 at.% to 50 at.% Mg (Figure 13) was determined by differential thermal analyses, X-ray diffraction and metallography. The  $T_0$  curve was determined by using the model proposed by Herchenroeder [5] for the rare earth - Mg systems. Due to the low heat involved for the  $\alpha/\alpha + \text{MMg}$  and  $\alpha/\alpha + \beta$  phase boundaries, these lines were determined by X-ray and metallographic methods, respectively.

The  $\alpha/\alpha + \beta$  solvus line was determined by microscopic examination of quenched alloys as described by Hume-Rothery et al. [15]. Several

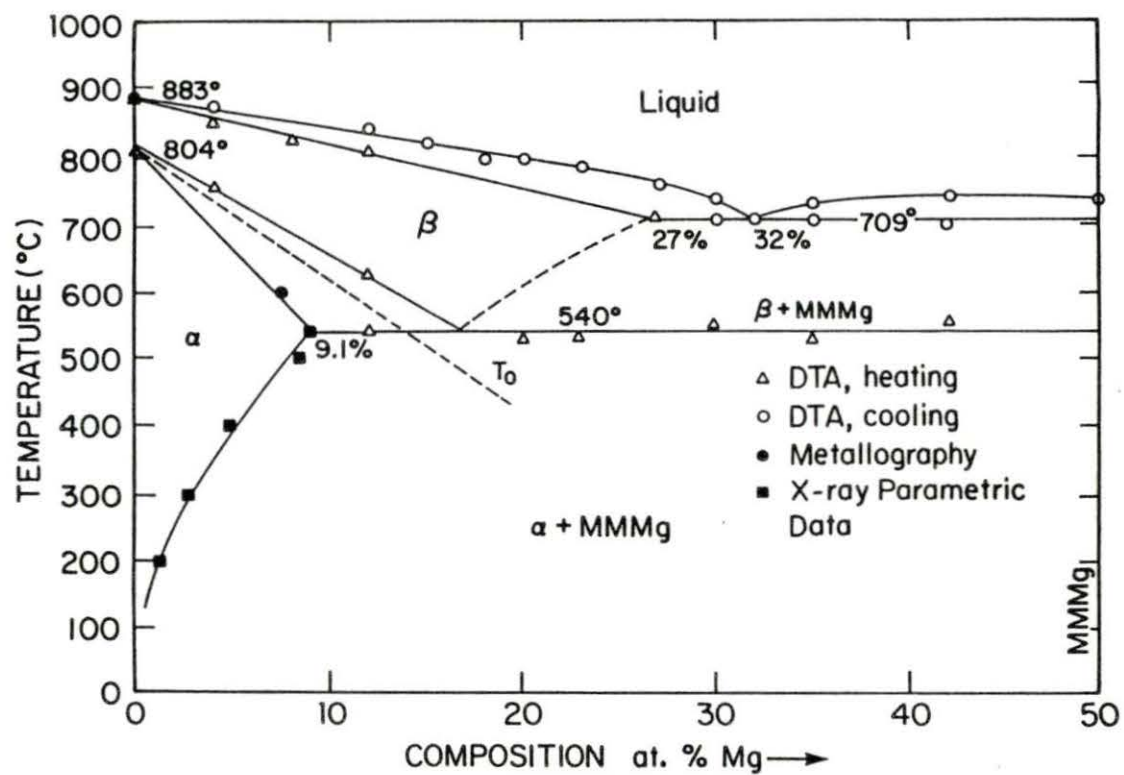


Figure 13. Mischmetal - magnesium phase diagram (0-50 at.% Mg)

samples of MM - Mg alloys (2 at.% Mg, 4 at.% Mg, 6 at.% Mg and 8 at.% Mg) were annealed for 48 hours at two different temperatures (700°C and 600°C) and then quenched in a ice-water-acetone bath. By metallographic observation, the maximum solubility of magnesium in the  $\alpha$  (dhcp) phase was determined for each temperature. As can be seen in Figures 14 and 15, the magnesium maximum solubility occurs between the two compositions in which the microstructures of adjacent compositions show a single-phase alloy and a two-phase alloy. For 600°C, this occurs between 6 and 8 at.% Mg and for 700°C, between 4 and 6 at.% Mg.

The  $\alpha/\alpha + \text{MMg}$  phase boundary was determined by using the X-ray parametric method [14]. First, a series of MM - Mg alloys (0 at.% Mg, 3 at.% Mg, 6 at.% Mg, 8 at.% Mg, 9 at.% Mg and 12 at.% Mg) were melted, slow cooled to 500°C, annealed at this temperature for one week and then ice quenched. From X-ray diffraction (Figures 16-21), the lattice parameters for the resulted  $\alpha$  (dhcp) structure were calculated (Table 4), the two lattice parameters (a and c) were plotted against magnesium composition (Figures 22 and 23) and from the intercepts of the two straight lines, the value for the solubility of

Table 4. Lattice parameters for MM - Mg alloys quenched from 500°C

	Mg (at.%)					
	0	3	6	8	9	12
$a(\text{\AA})$	$3.718 \pm 2$	$3.693 \pm 3$	$3.684 \pm 8$	$3.677 \pm 2$	$3.670 \pm 2$	$3.670 \pm 4$
$c(\text{\AA})$	$11.99 \pm 2$	$11.87 \pm 2$	$11.84 \pm 4$	$11.85 \pm 4$	$11.82 \pm 2$	$11.82 \pm 2$



(a)



(b)



(c)

Figure 14. Optical micrographs quenched from 600°C for (a) alloy MM - 4 Mg (100X), (b) alloy MM - 6 Mg (100X) and (c) alloy MM - 8 Mg (100X)

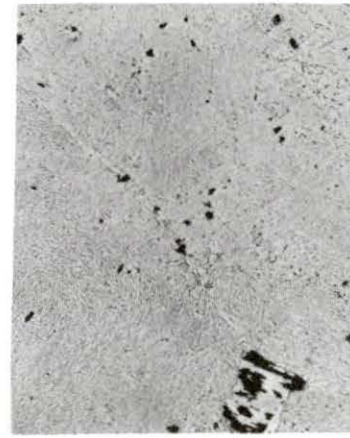




(a)



(b)



(c)

Figure 15. Optical micrographs quenched from 700°C for (a) alloy MM - 2 Mg (100X), (b) alloy MM - 4 Mg (200X) and (c) alloy MM - 6 Mg (200X)

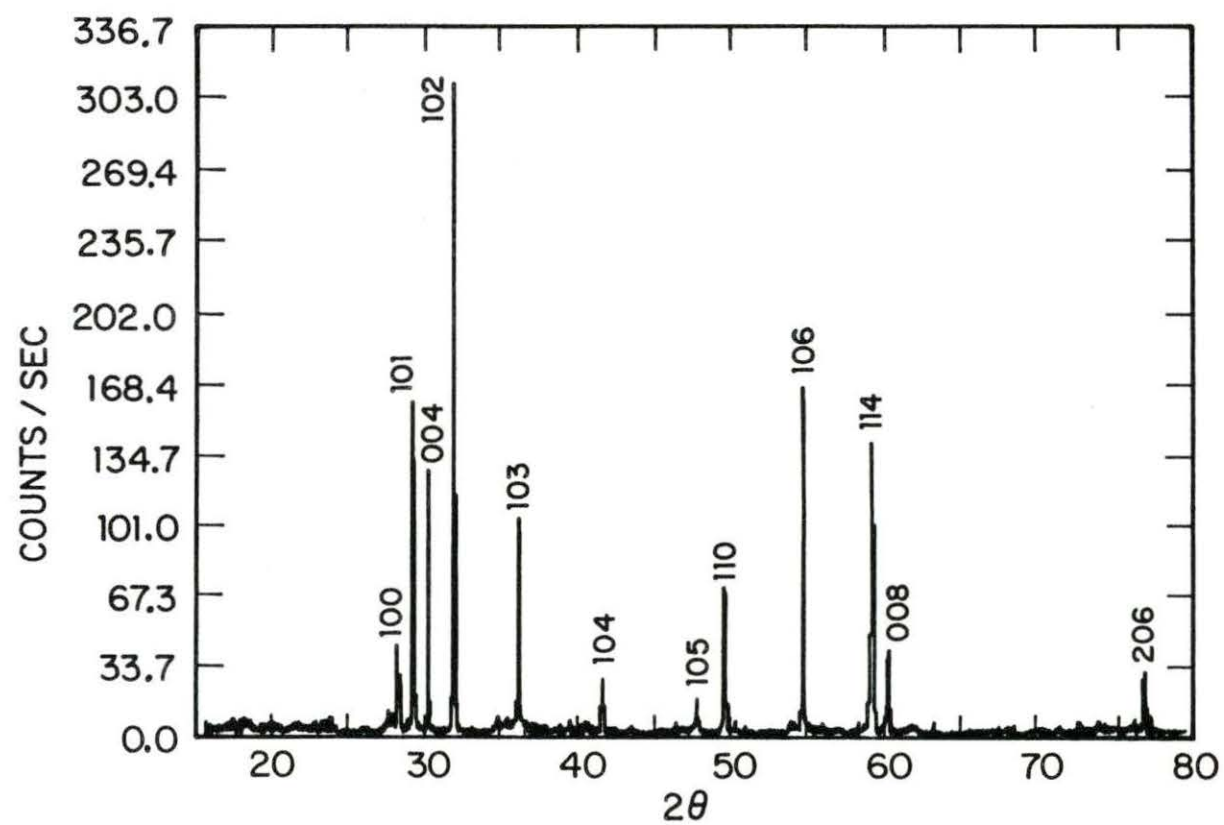


Figure 16. X-ray pattern of pure mischmetal quenched from 500°C

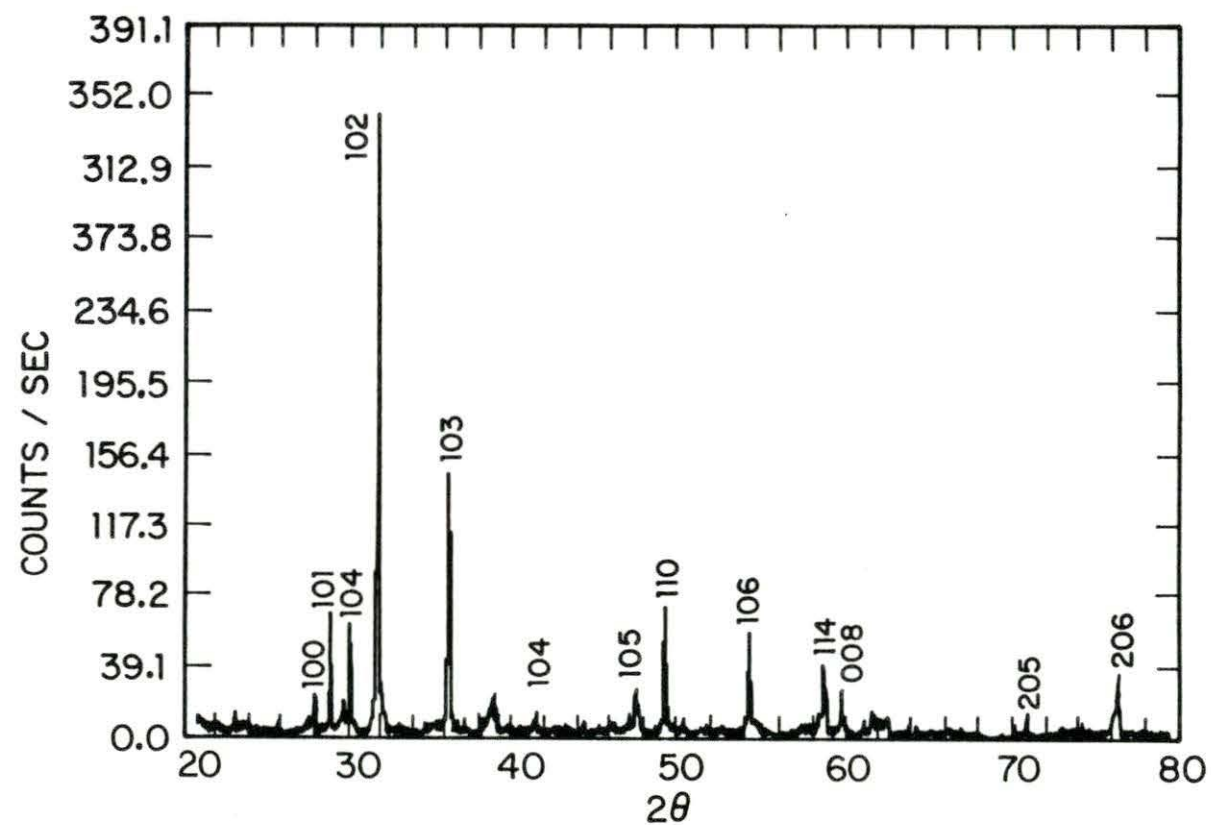


Figure 17. X-ray diffraction pattern of MM - 3 Mg alloy quenched from 500°C

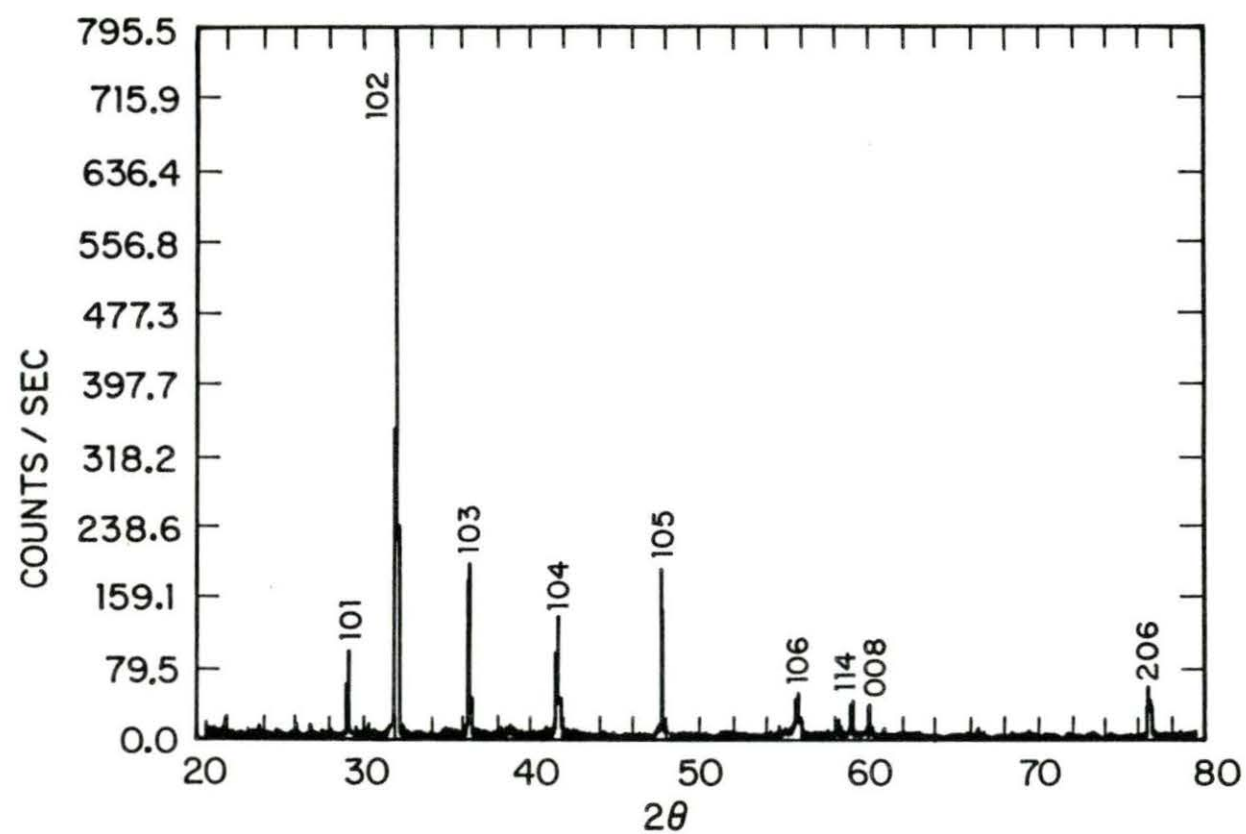


Figure 18. X-ray diffraction pattern of MM - 6 Mg alloy quenched from 500°C

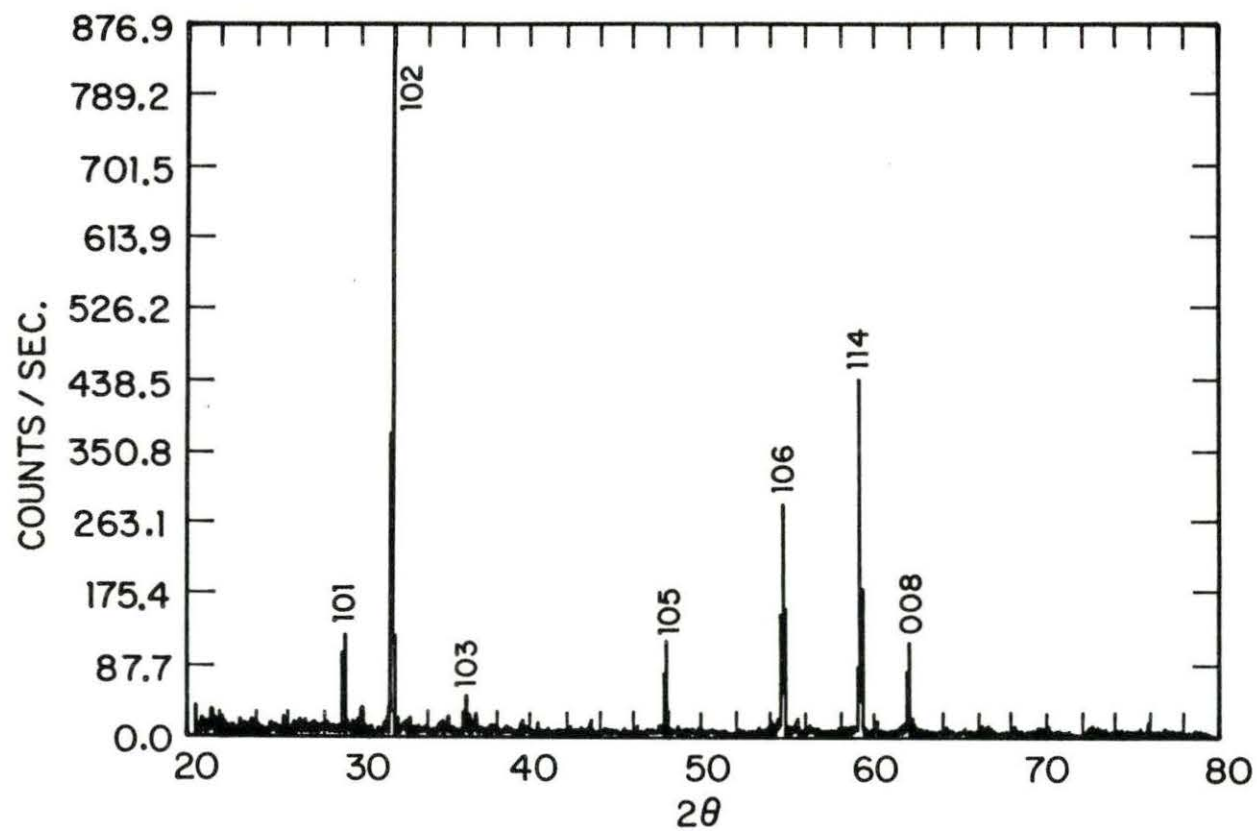


Figure 19. X-ray diffraction pattern of MM - 8 Mg alloy quenched from 500°C

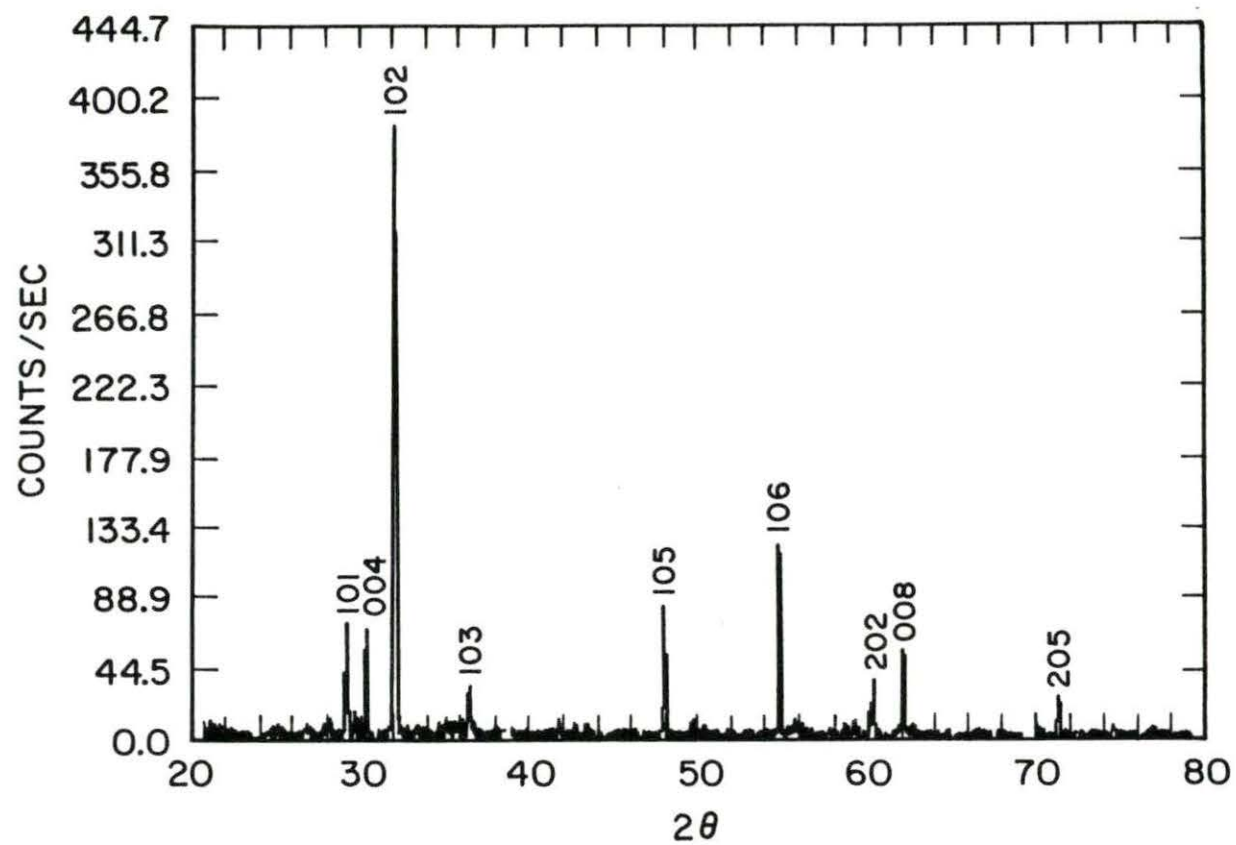


Figure 20. X-ray diffraction pattern of MM - 9 Mg alloy quenched from 500°C

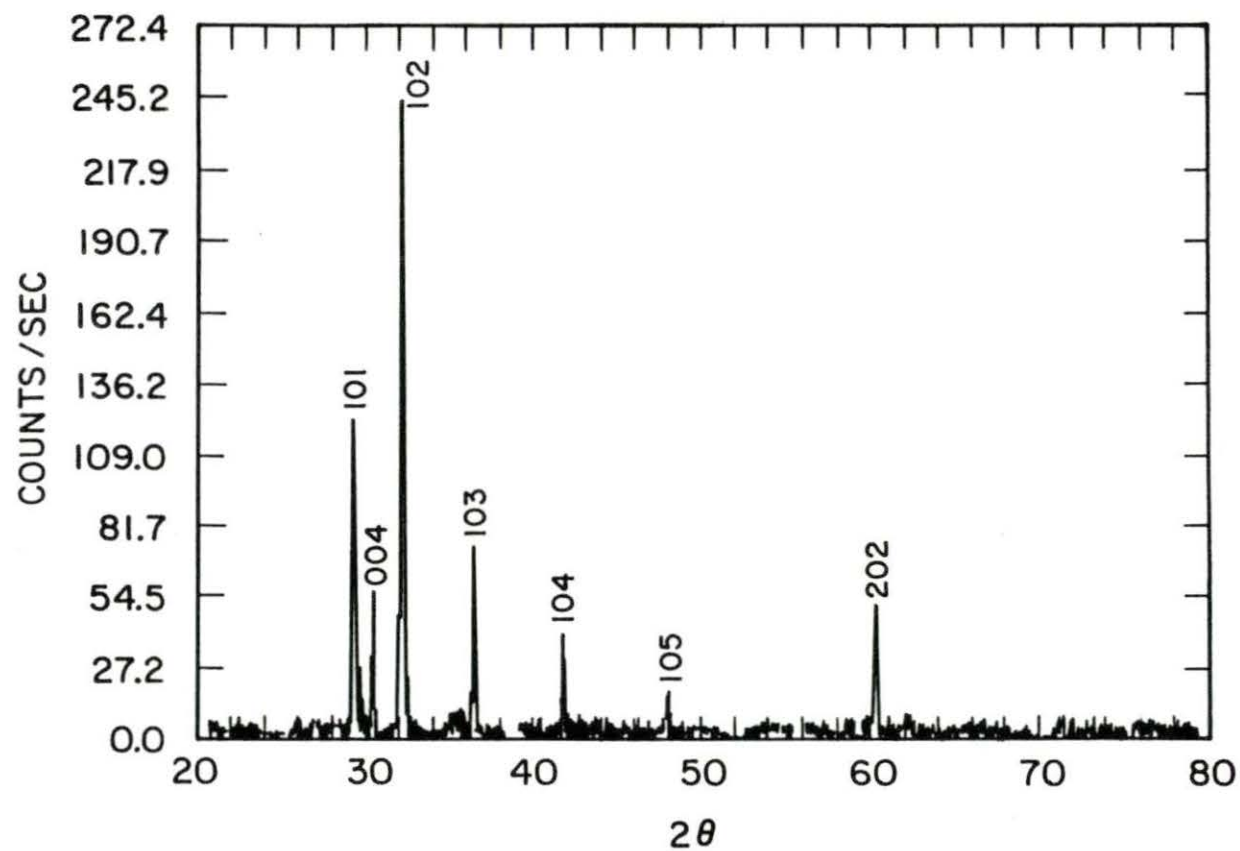


Figure 21. X-ray diffraction pattern of MM - 12 Mg alloy quenched from 500°C



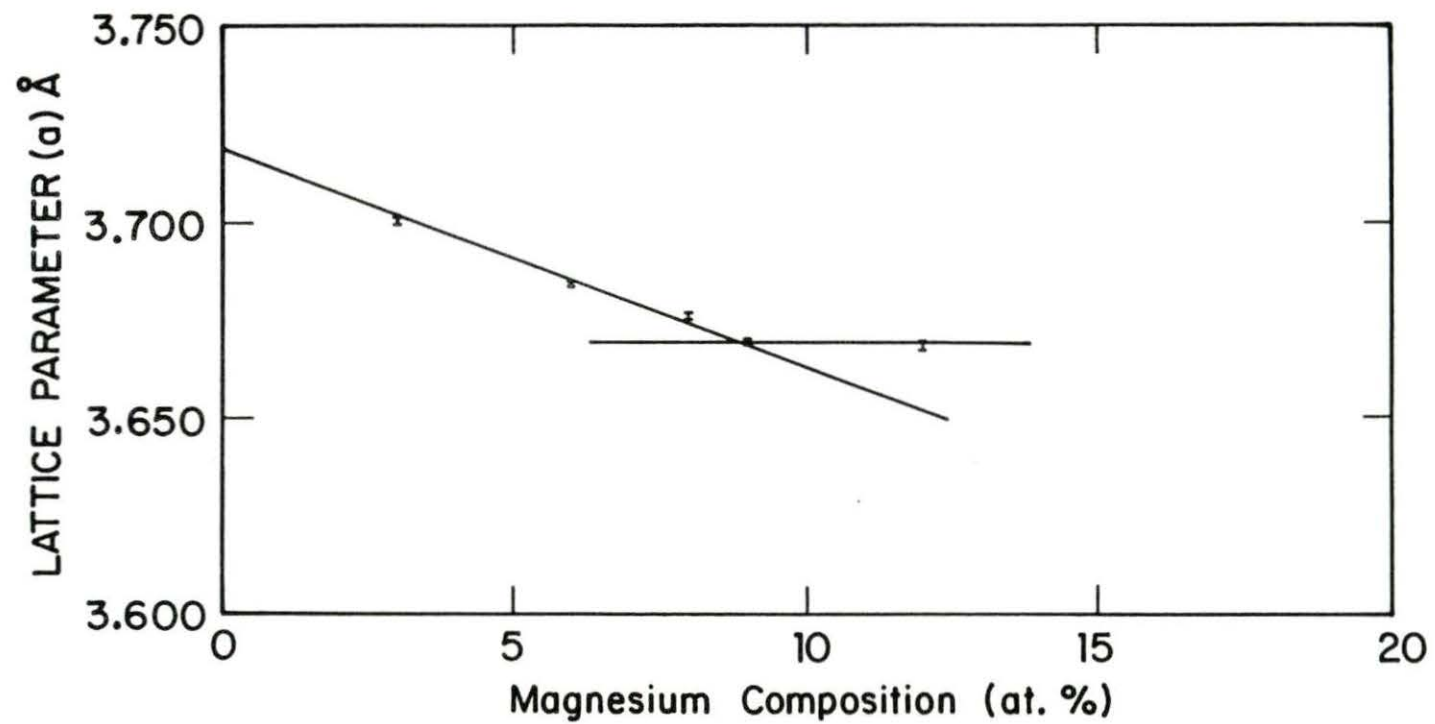


Figure 22. Lattice parameters ( $a$ ) for the MM - Mg samples quenched from several temperatures

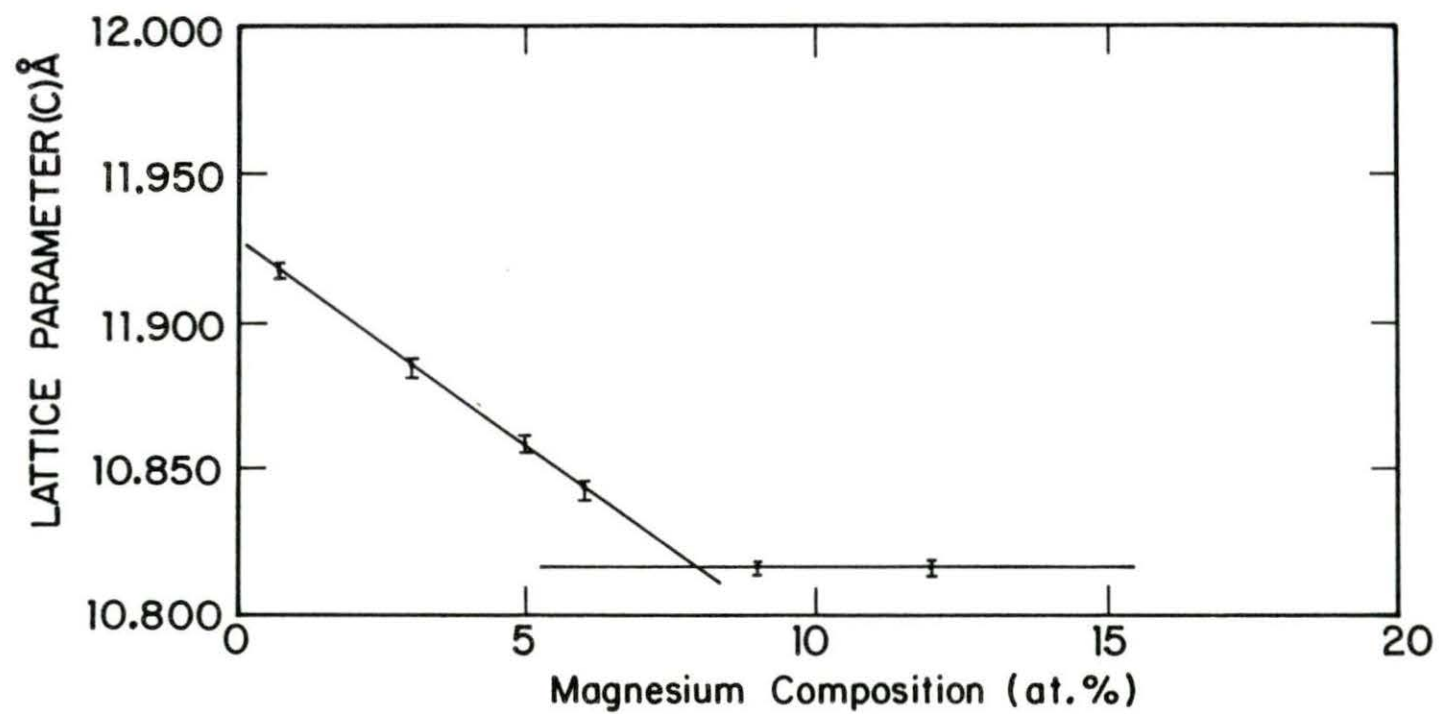


Figure 23. Lattice parameters ( $c$ ) for the MM - Mg samples quenched from several temperatures

Mg in  $\alpha$  at 500°C was found to be  $8.6 \pm 0.5$  at.%. To determine the solubility limit at other temperatures, several samples of MM - 9 at.% Mg were melted, slowly cooled to three different temperatures (250°C, 300°C and 400°C), annealed for two weeks and finally, ice quenched. The resulting lattice parameters (the X-ray diffraction patterns can be seen in Figures 24-26, respectively) are given in Table 5. From Figures 22 and 23, the maximum solid solubility of Mg in  $\alpha$  (dhcp) was determined, for each of these temperatures, by simply intersecting the lattice parameters shown in Table 5 with the inclined straight line of Figures 22 and 23. Table 6 shows the results. The maximum solid solubility of Mg in  $\alpha$  at the eutectoid transformation temperature was found by plotting the natural logarithm of the maximum magnesium composition at each temperature ( $\ln x$ ) against the inverse of the corresponding temperature ( $1/T$ ) (Figure 27). From the intersection of the inverse of eutectoid temperature with the  $\ln x$  vs.  $1/T$  plot, the composition was determined to be  $\sim 9.1 \pm 0.5$  at.% Mg. It was not possible to determine the  $\beta \rightarrow \beta + \text{MMMg}$  line due to the sluggish character of this transformation, even at extremely slow rates of heating and cooling. All the other lines were determined by D.T.A. and the error associated to them was about  $\pm 3^\circ\text{C}$ .

The addition of magnesium expanded the  $\beta(\text{bcc})$  region and lowered the  $\beta \rightarrow \alpha$  transformation temperature from 804°C to about 540°C and resulted in an eutectoid point at  $\sim 17$  at.% Mg. The maximum solid solubility of Mg in the dhcp and the bcc phases occurs at  $\sim 9.1$  at.% Mg at 540°C and  $\sim 27$  at.% Mg at 709°C, respectively. The critical  $T_0$

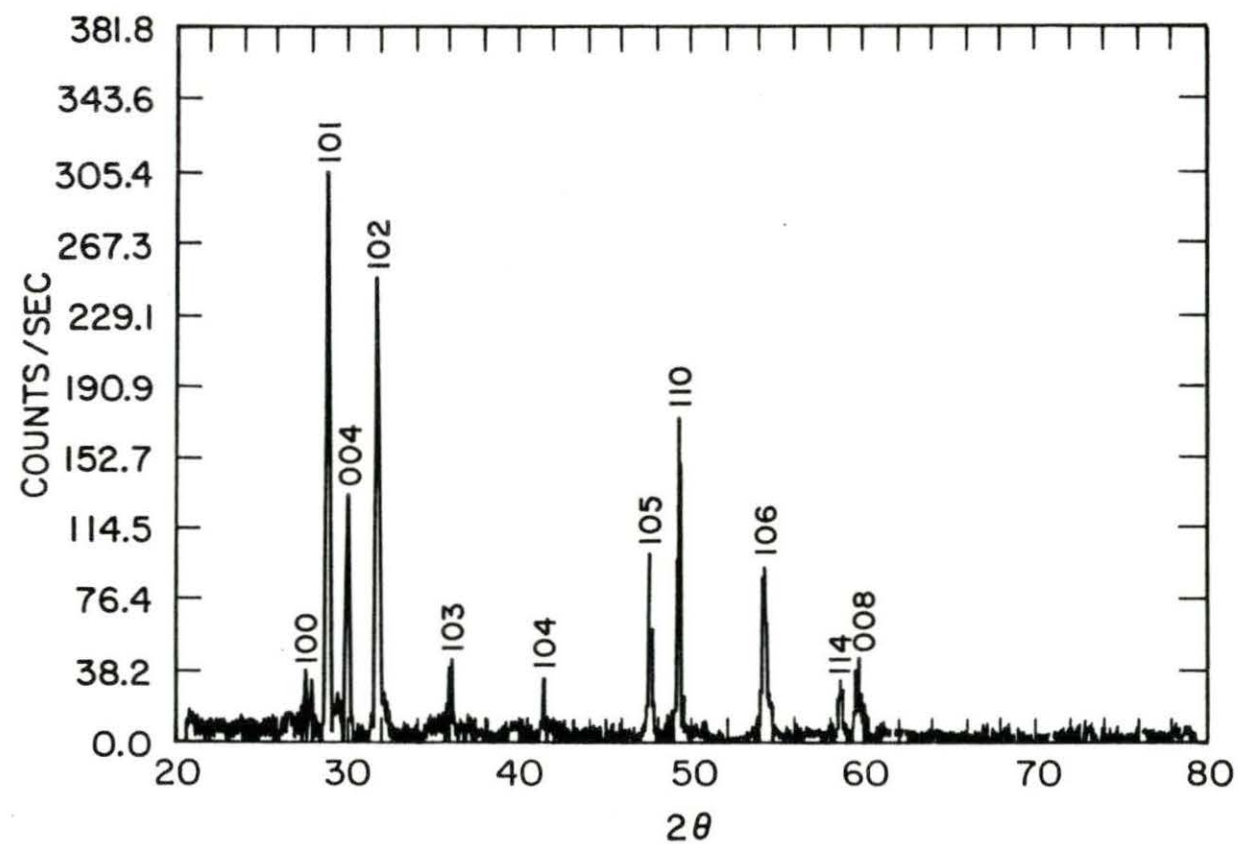


Figure 24. X-ray diffraction pattern for sample MM - 9 Mg quenched from 250°C

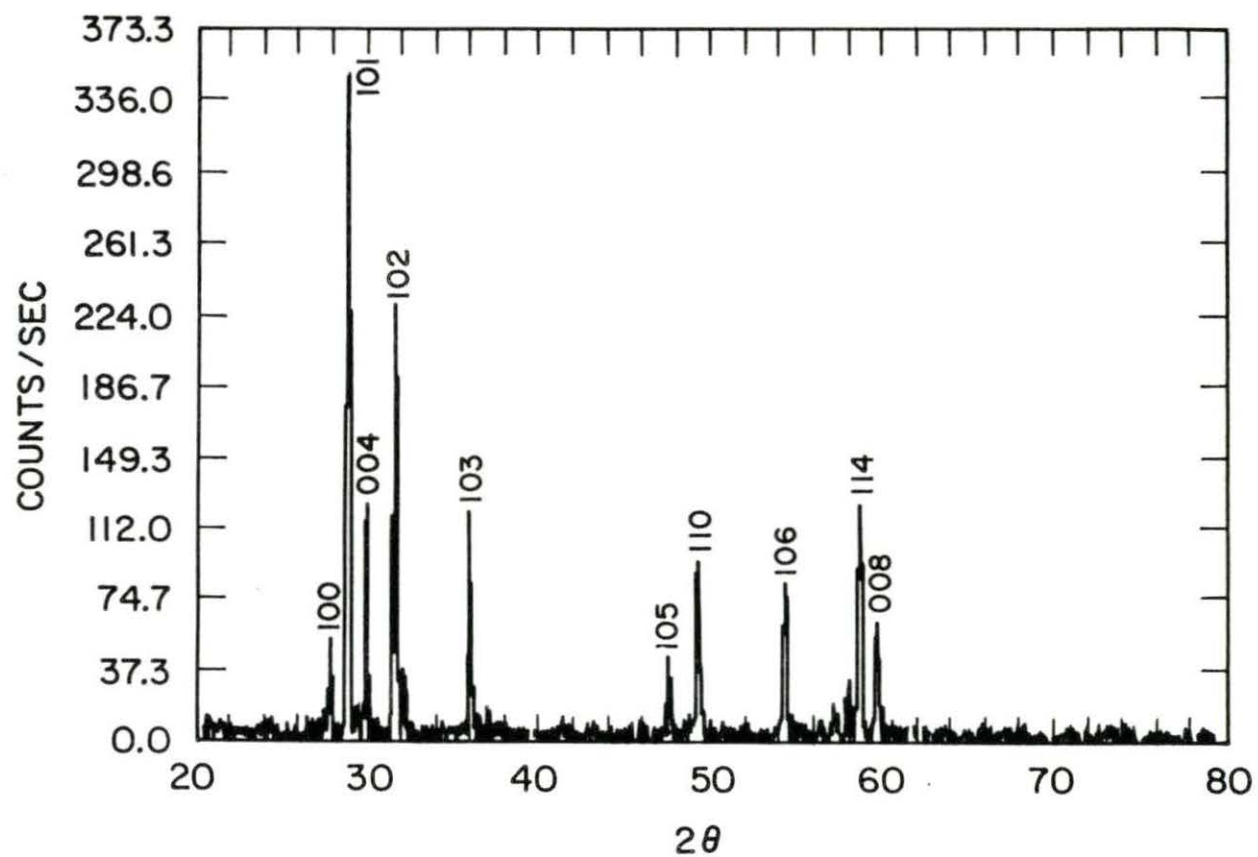


Figure 25. X-ray diffraction pattern for sample MM - 9 Mg quenched from 300°C

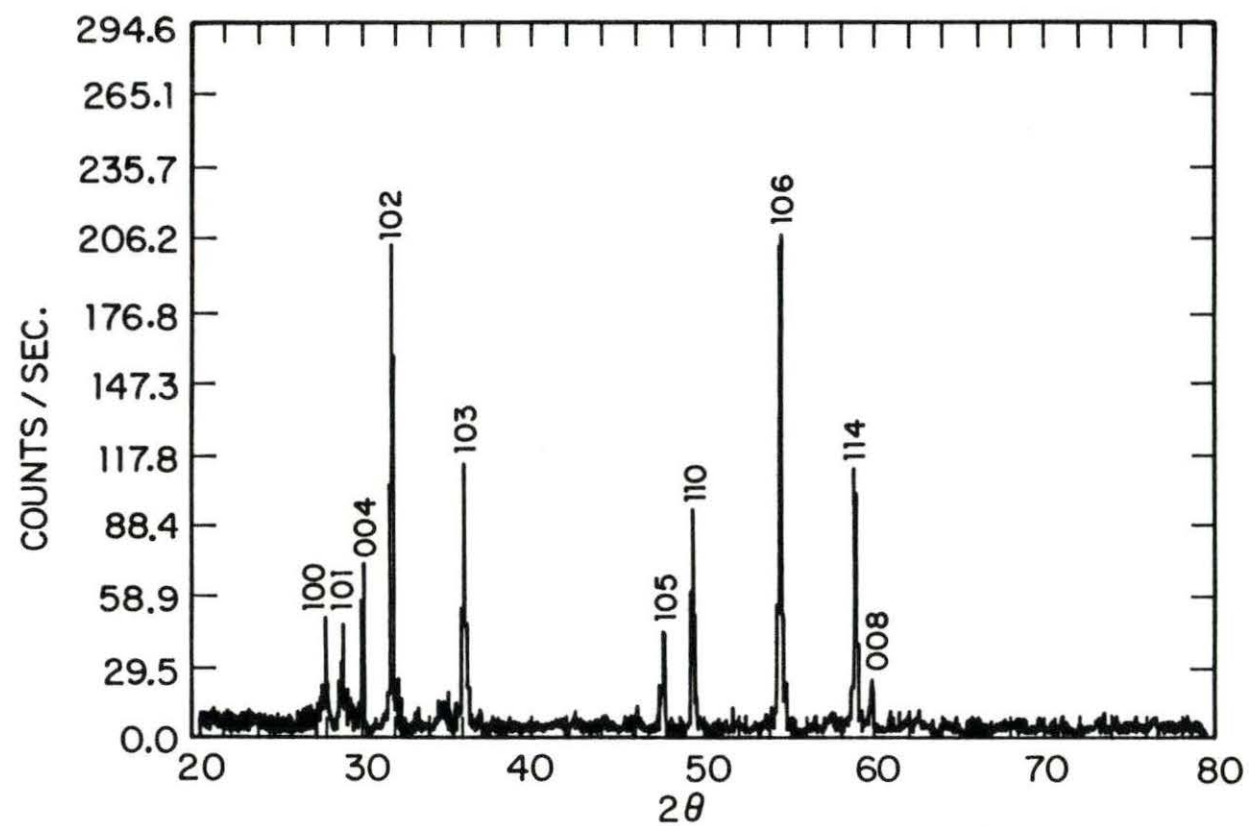


Figure 26. X-ray diffraction pattern for sample MM - 9 Mg quenched from 400°C

Table 5. Lattice parameter for sample MM - Mg quenched from different temperatures

	Quenching temperatures (°C)		
	400	300	250
a (Å)	3.691 $\pm$ 1	3.702 $\pm$ 1	3.701 $\pm$ 4
c (Å)	11.87 $\pm$ 1	11.92 $\pm$ 2	11.93 $\pm$ 4

Table 6. Maximum solid solubility of magnesium in  $\alpha$ 

	Temperature (°C)				
	540	500	400	300	250
Maximum solubility of Mg (at.%)	9.1 $\pm$ 0.5	8.6 $\pm$ 0.5	5.0 $\pm$ 0.5	3.0 $\pm$ 0.5	1.4 $\pm$ 0.5

temperature was found to be about  $\sim 500^{\circ}\text{C}$ , which is close to the  $515^{\circ}\text{C}$  found by Herchenroeder [5].



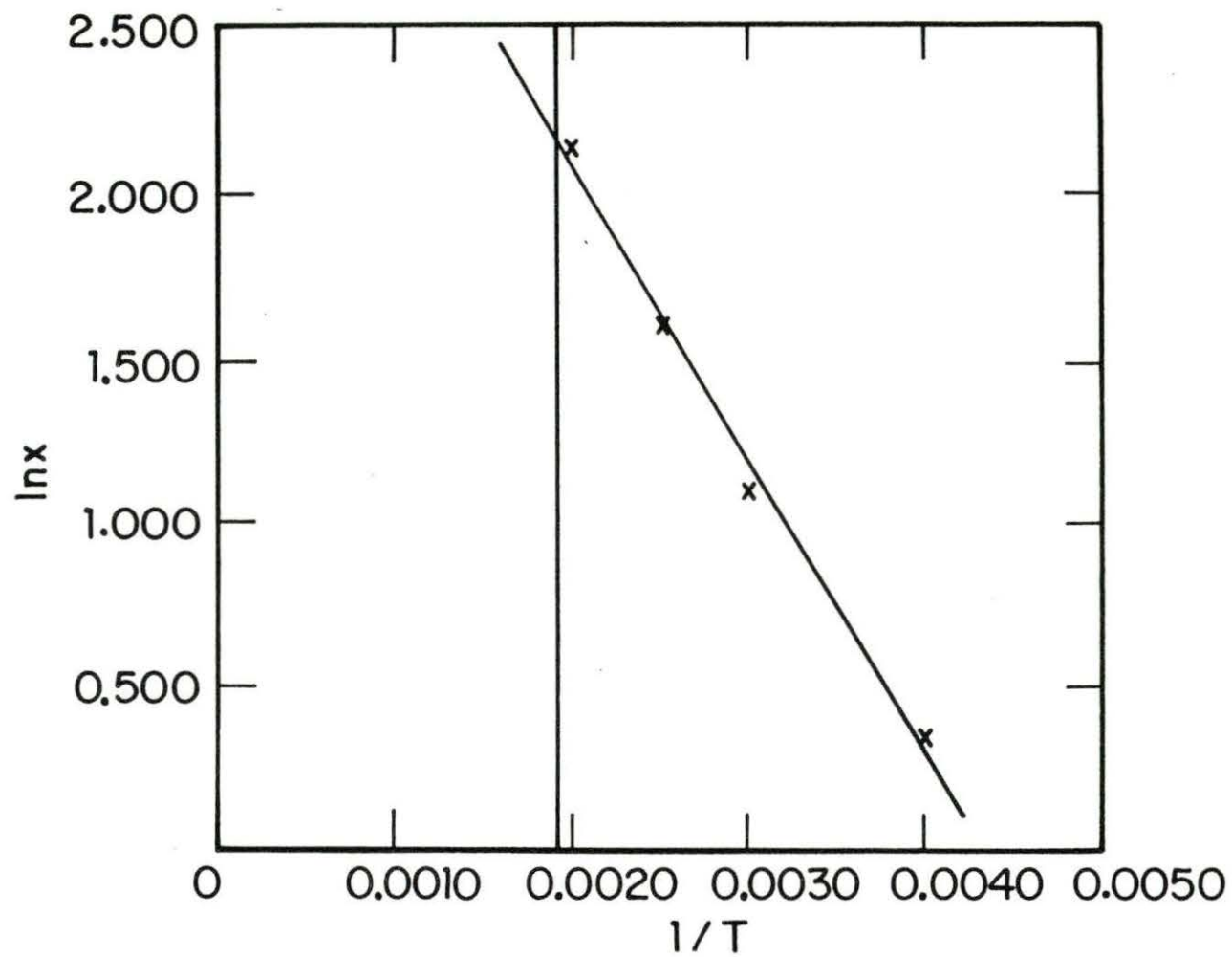


Figure 27. Determination of magnesium solid solubility ( $x$ ) in dhcp phase at the eutectoid temperature

## DISCUSSION

The magnesium composition range suitable for retaining the bcc phase was the same as that found for the lanthanum-magnesium system. In both systems, the alloys were quenched in ice-water-acetone baths, as described by Herchenroeder [5]. The other light lanthanide systems, Ce-Mg, Pr-Mg and Nd-Mg, have not been studied, but the phase diagrams are known [9]. For these systems, the magnesium maximum solid solubility in the bcc phase ( $27 \text{ at.}\% \pm 2 \text{ Mg}$ ), the eutectoid transformation temperature ( $510^\circ\text{C} \pm 30$ ), and the shape of the phase diagram are similar to that of the La-Mg system. Thus, it is reasonable to predict that the bcc retainability behavior between mischmetal-magnesium and La-Mg, Ce-Mg, Nd-Mg, Pr-Mg is about the same for all of the systems. Quenching from the bcc solid state was not attempted because the cooling rate during the time the sample is removed from the furnace is sufficiently slow for the equilibrium transformation to begin. The 16 at.% Mg alloy was the lowest possible composition for which we were able to retain 100% bcc. By increasing the quenching rate, this composition limit can be lowered, but changing the rate of quench was beyond the scope of this study.

For the sample MM - 15 Mg, some bcc was retained (Figure 2), but the quench rate was not sufficiently fast enough to reach the critical temperature necessary to prevent the  $\text{bcc} \rightarrow \text{dhcp} + \text{MMg}$  transformation from beginning. At a higher composition (21 at.% Mg), the bcc retention was limited by the precipitation of the intermetallic

compound  $\text{MMg}$  (Figure 3). Even though, the  $T_0$  curve drops to lower values at high solute composition due to high free energy of formation of  $\text{MMg}$ .

The bcc MM - 18 Mg sample presented the sharpest peaks for its X-ray diffraction pattern (Figure 5), as should be expected because of its closeness to the eutectoid point. At lower composition (16 at.% Mg), line broadening of the X-ray peaks was observed (Figure 4). This line broadening was an indication that the quench rate started to be critical at this composition.

The  $T_0$  critical point ( $T_{0,c}$ ) was determined to be  $\sim 500^\circ\text{C}$ . According to the proposal of Herchenroeder and Gschneidner [1], the bcc phase should not be retained in this system because  $T_{0,c} < T_{\text{eutectoid}} \approx 540^\circ\text{C}$ . However, two important factors override this criteria in this system. A strong undercooling of about  $40^\circ\text{C}$  observed in the D.T.A. even at slow cooling rates, and the big size difference between the MM and Mg atoms suggested that Mg is a slow diffuser. Because of this, the equilibrium reaction ( $\text{bcc} \rightarrow \text{dhcp} + \text{MMg}$ ) is sluggish, allowing the bcc retention.

As was expected, the addition of Mg to MM caused the lattice parameter of the bcc MM-Mg alloys to decrease. A good agreement was observed between the theoretical and experimental values for the bcc pure mischmetal lattice parameter. Antiferromagnetic ordering at low temperatures is common behavior for Ce, Pr and Nd (La is paramagnetic and superconducts at 5 or 6 K, depending upon the crystal structure). The value of bcc MM-Mg alloys determined experimentally for the

effective magnetic moment was in good agreement with the theoretical value. The observed decrease in the Curie-Weiss temperature with increasing magnesium content is due to magnetic dilution.

The MM rich end of the MM-Mg phase diagram was found to be similar to the La-Mg, Ce-Mg and Pr-Mg systems. The values for the equilibrium transformation temperature were registered during heating because of the strong undercooling effect observed in alloys which had compositions around the eutectoid point. The values of the energy of transformation for the bcc  $\rightarrow$  dhcp reaction were calculated from the values for the individual elements (La, Ce, Pr and Nd) given by Gschneidner [8].

## CONCLUSIONS

The bcc phase in the MM-Mg system can be metastably retained at room temperature for magnesium composition within the range 16 at.% - 20 at.%. The retention of a lower composition was restricted by quenching rate and at higher concentrations by intermetallic compound precipitation.

The lattice parameter for the pure bcc mischmetal phase was determined by extrapolation. The value obtained ( $a_E = 4.131 \text{ \AA}$ ) was in good agreement with the theoretical value ( $a_t = 4.156 \text{ \AA}$ ). Magnetic susceptibility data suggested that bcc mischmetal-magnesium alloys underwent a change from paramagnetic to antiferromagnetic behavior on cooling at  $\sim 20 \text{ K}$ , independent of magnesium composition. The value found for the magnetic effective moment per gram-atom-magnetic-rare earth of each bcc MM-Mg alloy examined (MM - 16 Mg, MM - 18 Mg and MM - 20 Mg) was found to be constant ( $p_{\text{eff}} \approx 1.62 \mu_B$ ), independent of the magnesium composition. The observed Curie-Weiss temperature values decreasing with the magnesium content increasing were due to magnetic dilution.

The equilibrium reaction  $\text{bcc} \rightarrow \text{dhcp} + \text{MMg}$  presented an undercooling effect of  $\sim 40^\circ\text{C}$  around the eutectoid composition ( $\sim 17 \text{ at.\% Mg}$ ). The sluggish character of this reaction was considered the strongest effect for the bcc structure retention in the mischmetal-magnesium system.



## REFERENCES

1. Herchenroeder, J. W.; Gschneidner, K. A., Jr. Bulletin of Alloy Phase Diagrams 1988, 9, 2.
2. Gibson, E. D.; Carlson, O. N. Trans. Am. Soc. Metals 1960, 52, 1047.
3. Miller, A. E.; Daane, A. H. Trans. Met. Soc. AIME 1964, 230, 568.
4. Manfrinetti, P.; Gschneidner, K. A., Jr. J. Less-Common Metals 1986, 123, 267.
5. Herchenroeder, J. W. Ph.D. Dissertation, Iowa State University, Ames, IA, 1988.
6. Fishman, S. G.; Crowe, C. R. J. Less-Common Metals 1972, 29, 253.
7. Palmer, P. E.; Burkholder, H. R.; Beaudry, B. J.; Gschneidner, K. A., Jr. J. Less-Common Metals 1982, 87, 135.
8. Gschneidner, K. A., Jr. "Physical properties of the rare earth metals"; U.S. Atomic Energy Commission Report Number IS-J2749; Rare-Earth Information Center, Ames Laboratory, Iowa State University, Ames, IA.
9. Gschneidner, K. A., Jr. Rare Earth Alloys; D. Van Nostrand Company, Inc.: New York, 1961.
10. Miller, A. E.; Daane, A. H.; Habermann, C. F.; Beaudry, B. J. Rev. Sci. Instr. 1963, 34, 644.
11. Peterson, D. T.; Hopkins, E. N. U.S. Atomic Energy Commission Report Number IS-1036; Ames Laboratory, Iowa State University, Ames, IA.
12. Croat, J. J. Ph.D. Dissertation, Iowa State University, Ames, IA, 1972.
13. Spedding, F. H.; Sanden, B.; Beaudry, B. J. J. Less-Common Metals 1973, 31, 1.
14. Cullity, B. D. Elements of X-ray Diffraction, 2nd ed.; Addison-Wesley Publishing Company, Inc.: Menlo Park, CA, 1978.
15. Hume-Rothery, W.; Christian, J. W.; Pearson, W. B. Metallurgical Equilibrium Diagrams; Unwin Brothers Limited: London, 1952.

16. Teatum, E. T.; Gschneidner, K. A., Jr.; Waber, J. T. "Compilation of calculated data useful in predicting metallurgical behavior of the elements in binary alloy systems"; Report Number LA-4003; Los Alamos Scientific Laboratory, University of California, Los Alamos, NM, 1968.



## ACKNOWLEDGMENTS

To achieve a graduate degree is not an easy task. I could not have gone through it without emotional and financial support from my wonderful parents and Godparents.

During this work compilation, I realized how important it is to have an excellent major professor, Dr. Karl Gschneidner, Jr., who allowed me to have my own ideas and judgements, and made me grow as a professional and a person. I will always be thankful for this.

Many other people have made contributions to this work and should be mentioned: Jim Herchenroeder helped me to get started; Jack Moorman, Paul Palmer, Nile Beymer, Harlan Baker, Bruce Cook, Jinke Tang, Jennings "Cap" Capellen and Michael Damento for their technical help and fruitful discussions.

This work was performed at Ames Laboratory under Contract No. W-7405-eng-82 with the U.S. Department of Energy. The United States government has assigned the DOE report number IS-T1392 to this thesis.

## APPENDIX A: MISCHMETAL CHEMICAL COMPOSITION (at.%)

La <sup>a</sup>	Ce <sup>a</sup>	Pr <sup>a</sup>	Nd <sup>a</sup>	Sm <sup>a</sup>	Gd <sup>a</sup>	Y <sup>a</sup>	Fe <sup>b</sup>	Mg <sup>c</sup>	Si <sup>c</sup>
43.2	42.0	6.4	8.4	<0.5	<0.2	<0.05	0.003	<0.001	<0.0001

Nonmetallic impurity contents (at. ppm):

H	C	N	O	F
139	47	10	175	66

---

<sup>a</sup>Determined by flame emission spectroscopy.

<sup>b</sup>Determined by visible spectrophotometry.

<sup>c</sup>Determined by spark source mass spectrometry.

## APPENDIX B: ALLOY CALCULATION

The magnesium atomic mole fraction is given by

$$x_{\text{Mg}} = \frac{n_{\text{Mg}}}{n_{\text{Mg}} + n_{\text{MM}}} \quad (1)$$

where

$n_{\text{Mg}}$  = number of g-atom of magnesium and

$n_{\text{MM}}$  = number of g-atom of mischmetal.

Substituting

$$n_i = \frac{\omega_i}{m\omega_i}$$

in Eq. (1) where  $\omega_i$  is the weight of the  $i$ th element and  $m\omega_i$  is the molecular weight of the  $i$ th element gives

$$x_{\text{Mg}} = \frac{\omega_{\text{Mg}}}{\omega_{\text{Mg}} + \left( \frac{m\omega_{\text{Mg}}}{m\omega_{\text{MM}}} \right) \omega_{\text{MM}}}$$

Alloy composition (atomic percent of magnesium):

<u>Designated</u>	<u>Actual</u>
MM - 15 Mg	14.98
MM - 16 Mg	16.28
MM - 18 Mg	18.02
MM - 20 Mg	20.40
MM - 21 Mg	20.97

## APPENDIX C: CALCULATED PURE BCC MISCHMETAL LATTICE PARAMETER

Based on the mischmetal chemical composition (at.%), an average metallic radius can be evaluated as follows:

Element	Metallic radius (Å) <sup>1</sup> C.N. = 12 <sup>2</sup>	Mischmetal chemical composition (at.%)
La	1.8791	43.2
Ce	1.8321	42.0
Pr	1.8279	6.4
Nd	1.8214	8.4

Then, the mischmetal average metallic radius (A.M.R.) will be:

$$\begin{aligned} \text{Mischmetal}_{\text{A.M.R.}} &= (1.8791 \times 0.432) + (1.8321 \times 0.42) \\ &\quad + (1.8279 \times 0.064) + (1.8214 \times 0.084) \end{aligned}$$

Hence,

$$\text{Mischmetal}_{\text{A.M.R.}} = 1.8513 \text{ Å} \quad (\text{C.N.} = 12)$$

When transforming from dhcp (C.N. = 12) to bcc (C.N. = 8), a correction must be made to the metallic radius for the change in

---

<sup>1</sup>From Reference [8].

<sup>2</sup>C.N. is the coordination number.

coordination number. Teatum et al. [16] investigated the metallic elements that undergo the  $\text{bcc} \rightleftharpoons \text{fcc}$  or  $\text{dhcp}$  allotropy and determined an equation for this correction:

$$r_8 = 0.96937 r_{12} + 0.00516 \quad (2)$$

Assuming a good approach, Eq. (2) yielded

$$r_8 = 1.7998$$

for the mischmetal, and finally,

$$a = 4.156 \text{ \AA} \quad .$$